EUROPHYSICS LETTERS 15 May 2006

*Europhys. Lett.*, **74** (4), pp. 679–685 (2006)
DOI: 10.1209/epl/i2006-10024-x

# Spontaneous spin polarization in quantum wires

A. D. Klironomos, J. S. Meyer(*) and K. A. Matveev
*Materials Science Division, Argonne National Laboratory - Argonne, IL 60439, USA*

received 18 January 2006; accepted in final form 23 March 2006
published online 12 April 2006

PACS. 73.21.Hb – Quantum wires.
PACS. 75.10.Pq – Spin chain models.

**Abstract.** – A number of recent experiments report spin polarization in quantum wires in the absence of magnetic fields. These observations are in apparent contradiction with the Lieb-Mattis theorem, which forbids spontaneous spin polarization in one dimension. We show that sufficiently strong interactions between electrons induce deviations from the strictly one-dimensional geometry and indeed give rise to a ferromagnetic ground state in a certain range of electron densities.

Quantum wires are quasi-one-dimensional structures which, although conceptually simple, display extremely rich physics that defies conventional intuition developed for two- and three-dimensional conductors. The study of transport properties of quantum wires has offered a direct glimpse into the quantum world through the quantization of conductance in integer multiples of $G_0 = 2e^2/h$ [1]. Recently, one of the most exotic implications of one-dimensionality —the existence of separate spin and charge excitations— has been demonstrated experimentally [2].

In a number of recent experiments on quantum wires, deviations from perfect conductance quantization have been observed [3–11]. Most commonly, the experimental findings have been interpreted as indication of spontaneous spin polarization [3–8, 11–13]. However, for a strictly one-dimensional system this possibility is explicitly forbidden by a theorem due to Lieb and Mattis [14], based on very general mathematical properties of the Schrödinger equation describing these interacting electronic systems. Although a number of interpretations of the conductance anomalies that do not rely on the idea of spin polarization have been proposed [9, 10, 15–17], the experiments do raise a fundamental question: *Can the ground state of the electron system in a quantum wire be ferromagnetic?*

The only way to circumvent the Lieb-Mattis theorem is to recognize that realistic quantum wires are not in essence one-dimensional devices [18]. Attempts in that direction have been made [13], requiring, however, a fully two-dimensional structure as a starting point. By contrast, we start with the conventional model of an electron gas in a quantum wire and show that strong Coulomb interactions both cause deviations from one-dimensionality and bring about a ferromagnetic ground state.

(*) Present address: The Ohio State University, Columbus - OH 43210-1117, USA.

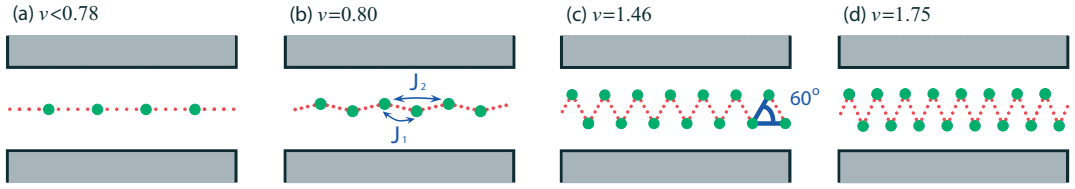


Fig. 1 – Wigner crystal of electrons in a quantum wire defined by gates (shaded). The structure is determined by the parameter $\nu$ proportional to electron density (see text). As density grows, the one-dimensional crystal (a) gives way to a zig-zag chain (b-d). The arrows in (b) illustrate the nearest-neighbor ($J_1$) and next-nearest-neighbor ($J_2$) exchange processes.

Typical experiments are done with quantum wires that are formed at the interfaces of GaAs/AlGaAs heterostructures. A voltage applied to metal gates provides a confining potential in the directions transverse to the wire and, in addition, allows one to tune the electron density in the wire. While conductance plateaus at integer multiples of $G_0$ are observed in the high-density regime, a drop in conductance commonly attributed [3–8] to spin polarization has been observed [3–9] in the region of gate voltages where the electron density is very low.

As the density $n$ of electrons is lowered, Coulomb interactions become more important, and at $n \ll a_B^{-1}$ they dominate over the kinetic energy. (Here $a_B = \hbar^2\epsilon/me^2$ is the Bohr radius in the material, $\epsilon$ is its dielectric constant, and $m$ is the effective electron mass; $a_B \approx 100\,\text{Å}$ in GaAs.) In this limit the electrons can be viewed as classical particles. In order to minimize their mutual Coulomb repulsion, electrons occupy equidistant positions along the wire, forming a structure with short-range crystalline order —the so-called Wigner crystal [21]. Upon increasing the density, the inter-electron distance diminishes, and the resulting stronger electron repulsion eventually overcomes the confining potential, transforming the classical one-dimensional Wigner crystal into a staggered or zig-zag chain [24]. Typical structures for different densities are shown in fig. 1.

Quantum-mechanically, spin-spin interactions in the Wigner crystal arise due to exchange processes, in which two electrons switch positions by tunneling through the potential barrier that separates them. The barrier is created by the two exchanging particles as well as all other electrons in the wire. Originating in tunneling, the exchange energy associated with such processes falls off exponentially with the distance between the electrons. As a result, only the nearest-neighbor exchange is relevant in a one-dimensional crystal. The corresponding exchange constant is positive, leading to an antiferromagnetic ground state in accordance with the Lieb-Mattis theorem [14].

A very different situation arises when one considers the most trivial deviation from the one-dimensional crystal, namely the zig-zag chain introduced above. For that structure, depending on the distance between the two rows which varies as a function of density, the distance between next-nearest neighbors may be equal to or even smaller than the distance between nearest neighbors, as illustrated in fig. 1(c,d). Accordingly, the next-nearest-neighbor exchange constant $J_2$ may be equal to or larger than the nearest-neighbor exchange constant $J_1$. The corresponding spin chain is described by the Hamiltonian

$$H_{12} = \sum_j \left(J_1 \boldsymbol{S}_j \boldsymbol{S}_{j+1} + J_2 \boldsymbol{S}_j \boldsymbol{S}_{j+2}\right). \tag{1}$$

The competition between the two exchanges causes frustration of the antiferromagnetic spin order and eventually leads to a gapped dimerized ground state at $J_2 > 0.24 J_1$, [25–27]. In

addition, drawing intuition from studies of the two-dimensional Wigner crystal, one realizes that in this geometry *ring-exchange* processes, in which three or more particles exchange positions in a cyclic fashion, have to be considered.

It has been established that, due to symmetry properties of the ground-state wave functions, ring exchanges of an even number of fermions favor antiferromagnetism, while those of an odd number of fermions favor ferromagnetism [28]. In a zig-zag chain, the Hamiltonian reads

$$H = \frac{1}{2}\sum_j \Big( J_1 P_{j\,j+1} + J_2 P_{j\,j+2} - J_3 (P_{j\,j+1\,j+2} + P_{j+2\,j+1\,j}) + J_4 (P_{j\,j+1\,j+3\,j+2} + P_{j+2\,j+3\,j+1\,j}) - \dots \Big), \tag{2}$$

where the exchange constants are defined such that all $J_l > 0$ and only the dominant $l$-particle exchanges are shown. Here, $P_{j_1 \dots j_l}$ denotes the cyclic permutation operator of $l$ spins. A more familiar form of the Hamiltonian in terms of spin operators is obtained using $P_{ij} = \frac{1}{2} + 2\boldsymbol{S}_i \boldsymbol{S}_j$ and $P_{j_1 \dots j_l} = P_{j_1 j_2} P_{j_2 j_3} \dots P_{j_{l-1} j_l}$ [28]. In particular, the two-spin exchanges reduce to eq. (1).

The simplest ring exchange involves three particles and is therefore ferromagnetic. Extensive studies of the two-dimensional Wigner crystal have shown that, at low densities (or strong interactions), the three-particle ring exchange dominates over the two-particle exchange. As a result, the two-dimensional Wigner crystal becomes ferromagnetic at sufficiently strong interactions [29, 30]. Since the electrons in a two-dimensional Wigner crystal form a triangular lattice, by analogy, one should expect a similar effect in the zig-zag chain at densities where the electrons form approximately equilateral triangles, fig. 1(c). In order to verify this scenario, we have to identify the electron configuration that is stable at a given density and subsequently find the corresponding exchange energies.

Specifically, we consider a quantum wire with a parabolic confining potential $V_{\rm conf}(y) = m\Omega^2 y^2/2$, where $\Omega$ is the frequency of harmonic oscillations in the potential $V_{\rm conf}(y)$. At low electron density $n$ in the wire, a one-dimensional Wigner crystal is formed, fig. 1(a). As the density grows, however, the Coulomb interaction energy becomes comparable to the confining potential, leading to the formation of a zig-zag chain, as depicted in fig. 1(b-d). This transition happens when distances between electrons are of the order of the characteristic length scale $r_0 = \left(2e^2/\epsilon m\Omega^2\right)^{1/3}$, such that $V_{\rm conf}(r_0) = V_{\rm int}(r_0)$, where $V_{\rm int}(r) = e^2/\epsilon r$ is the Coulomb interaction energy. It is convenient for the following discussion to introduce a dimensionless density $\nu = nr_0$. Minimization of the energy with respect to the electron configuration [24] reveals that a one-dimensional crystal is stable for densities $\nu < 0.78$, whereas a zig-zag chain forms at intermediate densities $0.78 < \nu < 1.75$. (At higher densities, the zig-zag chain gives way to structures with larger numbers of rows [24].) The distance between rows grows with density, and the equilateral configuration is achieved at $\nu \approx 1.46$, well within the region where the zig-zag chain is stable. Therefore, there are strong indications that the ferromagnetic state may be realized. More specifically, upon increasing the density one would expect the system to undergo two consecutive phase transitions: first from an antiferromagnetic to a ferromagnetic, and then to a dimer phase. However, the latter scenario cannot be established conclusively based solely on the two-dimensional Wigner crystal physics. The main differences are i) the presence of a confining potential as opposed to the flat background in the two-dimensional case, and even more importantly, ii) the change of the electron configuration with density, fig. 1, as opposed to the ideal triangular lattice in two dimensions. Below, we study numerically the exchange energies for the specific configurations of the zig-zag Wigner crystal in a parabolic confining potential.

The strength of the interactions is characterized by the parameter

$$r_\Omega = \frac{r_0}{a_B} = 2\left(\frac{me^4}{2\epsilon^2\hbar^2}\,\frac{1}{\hbar\Omega}\right)^{2/3}. \tag{3}$$

For $r_\Omega \gg 1$, the physics of the system is dominated by strong interactions, and a semiclassical description is applicable. In order to calculate the various exchange constants, we use the standard instanton method, also employed in the study of the two-dimensional Wigner crystal [29,31]. Within this approach, the exchange constants are given by $J_l = J_l^* \exp[-S_l/\hbar]$, where $S_l$ is the value of the Euclidean (imaginary time) action, evaluated along the classical exchange path. By measuring length and time in units of $r_0$ and $T = \sqrt{2}/\Omega$, respectively, the action $S[\{\boldsymbol{r}_j(\tau)\}]$ is rewritten in the form $S = \hbar\eta\sqrt{r_\Omega}$, where the functional

$$\eta[\{\boldsymbol{r}_j(\tau)\}] = \int_{-\infty}^{\infty} \mathrm{d}\tau \left[\sum_j \left(\frac{\dot{\boldsymbol{r}}_j^2}{2} + y_j^2\right) + \sum_{j<i} \frac{1}{|\boldsymbol{r}_j - \boldsymbol{r}_i|}\right] \tag{4}$$

is dimensionless.

Thus, we find the exchange constants in the form $J_l = J_l^* \exp[-\eta_l\sqrt{r_\Omega}]$, where the dimensionless coefficients $\eta_l$ depend only on the electron configuration (cf. fig. 1) or, equivalently, on density $\nu$. The instanton trajectories, and subsequently the exponents $\eta_l$, are calculated for each type of exchange by solving the equations of motion obtained from the dimensionless action (4) numerically.

To first approximation, we neglect the motion of all "spectators" —the electrons in the crystal to the left and to the right of the exchanging particles. The left panel of fig. 2 shows the calculated exponents for various exchanges as a function of dimensionless density $\nu$. At strong interactions ($r_\Omega \gg 1$), the exchange with the smallest value of $\eta_l$ is clearly dominant,

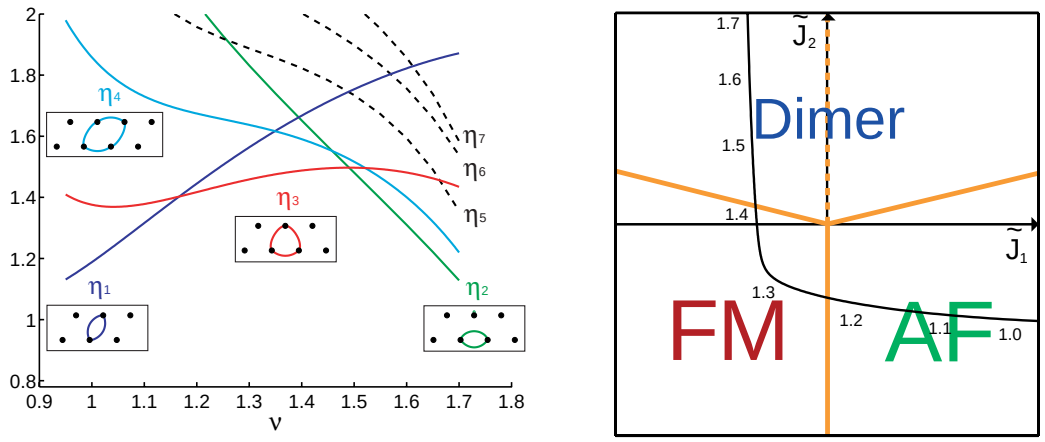


Fig. 2 – Left panel: the exponents $\eta_l$ as functions of the dimensionless density $\nu$, computed with frozen spectators. The insets illustrate the four most important exchange processes. Right panel: the phase diagram including nearest-neighbor, next-nearest-neighbor, and three-particle ring exchanges. The effective couplings $\widetilde{J}_1$ and $\widetilde{J}_2$ are defined in the text. The solid line shows schematically the traversal of the various phases with increasing dimensionless density $\nu$, as dictated by the calculated exchange energies.

and the prefactor $J_l^*$ is of secondary importance to our argument. The numerical calculation confirms our original expectation: the dominant exchange constant changes from nearest-neighbor exchange $J_1$ to three-particle ring exchange $J_3$ to next-nearest neighbor exchange $J_2$. More complicated ring exchanges have also been computed. The left panel of fig. 2 displays the ones with the smallest exponents, namely the four-particle ring exchange as well as five-, six-, and seven-particle ring exchanges (dashed lines).

If one includes only the dominant exchanges $J_1$, $J_2$, and $J_3$, the Hamiltonian of the corresponding spin chain takes a simple form. Nearest- and next-nearest-neighbor exchanges are described by eq. (1). Furthermore, the three-particle ring exchange does not introduce a new type of coupling, but modifies the two-particle exchange constants [28]. For a zig-zag crystal we find

$$H_3 = -J_3 \sum_j \left(2\boldsymbol{S}_j\boldsymbol{S}_{j+1} + \boldsymbol{S}_j\boldsymbol{S}_{j+2}\right). \tag{5}$$

Thus the total Hamiltonian still has the form (1), but with the effective two-particle exchange constants $\widetilde{J}_1 = J_1 - 2J_3$ and $\widetilde{J}_2 = J_2 - J_3$. Therefore, the regions of negative (*i.e.* ferromagnetic) nearest- and/or next-nearest-neighbor coupling become accessible. The phase diagram of the Heisenberg spin chain (1) with both positive and negative couplings is well studied [25–27, 32–35]. In addition to the antiferromagnetic and dimer phases discussed earlier, a ferromagnetic phase exists for $\widetilde{J}_1 < \max\{0, -4\widetilde{J}_2\}$ [33]. The phase diagram in terms of the effective exchange constants $\widetilde{J}_1$ and $\widetilde{J}_2$ is shown in the right panel of fig. 2. The solid line represents schematically the path followed in phase space, according to our numerical calculation of the exchange constants, as the density $\nu$ increases. At low densities, the system is close to one-dimensional and is, therefore, antiferromagnetic. In the range of densities corresponding to an "approximately equilateral" configuration, the three-particle ring exchange is strong, leading to a ferromagnetic ground state. Finally, at even higher densities, frustration caused by the next-nearest-neighbor coupling $J_2$ drives the system into a dimerized phase. (Note that there is some controversy concerning the physics of the parameter regime $-4\widetilde{J}_2 < \widetilde{J}_1 < 0$, where the existence of a spectral gap associated with dimerization has not yet been established conclusively [35].)

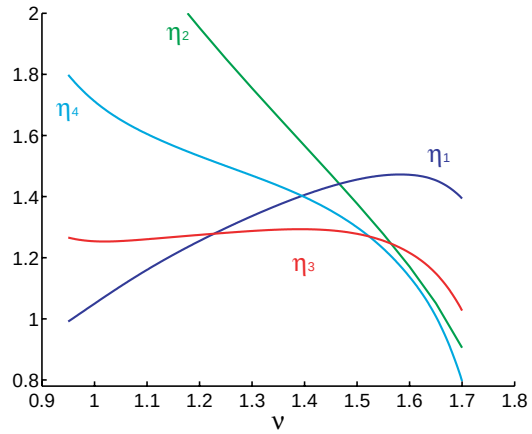


Fig. 3 – The exponents $\eta_1$, $\eta_2$, $\eta_3$, and $\eta_4$ as functions of the dimensionless density $\nu$. The computation includes 12 moving spectator particles on either side of the exchanging particles. Corrections to $\eta_l$ from the remaining spectators do not exceed 0.1%.

It turns out that the above picture, based on the calculation of the exponents to first approximation, is incomplete: because only the exchanging particles were allowed to move while all spectators were frozen in place, the values of $\eta_l$ were overestimated. Surprisingly, allowing spectators to move results not only in quantitative but in qualitative changes as seen in fig. 3 [23]. At large densities, the four-particle ring exchange $J_4$ dominates over $J_2$. Contrary to $J_3$, the four-particle ring exchange not only modifies the nearest- and next-nearest-neighbor exchange constants —in addition, it introduces more complicated spin interactions [28]. For the zig-zag chain, we find

$$H_4 = J_4 \sum_j \Big( \sum_{l=1}^{3} \frac{4-l}{2} \boldsymbol{S}_j \boldsymbol{S}_{j+l} + 2\big[ (\boldsymbol{S}_j \boldsymbol{S}_{j+1})(\boldsymbol{S}_{j+2} \boldsymbol{S}_{j+3}) + (\boldsymbol{S}_j \boldsymbol{S}_{j+2})(\boldsymbol{S}_{j+1} \boldsymbol{S}_{j+3}) - (\boldsymbol{S}_j \boldsymbol{S}_{j+3})(\boldsymbol{S}_{j+1} \boldsymbol{S}_{j+2}) \big] \Big). \tag{6}$$

Not much is known about the physics of zig-zag spin chains with interactions of this type. Preliminary numerical studies indicate that the ground state has zero magnetization [36]. Further work is required to identify the possibly novel spin structures. We would also like to point out that a confining potential of different shape might alter the outcome of the competition between the very close values of $\eta_4$ and $\eta_2$ at high densities.

In experiments with quantum wires, the interaction strength is not a tunable parameter: it is determined by the electron charge $e$ and the dielectric constant $\epsilon$ in the semiconductor host. However, the parameter $r_\Omega$ can still be tuned by adjusting the confining potential. As $r_\Omega \propto \Omega^{-2/3}$, making the confining potential more shallow effectively increases interaction effects. Quantum wires in semiconductor heterostructures are fabricated using either cleaved-edge-overgrowth or split-gate techniques. In cleaved-edge-overgrowth wires [2], we estimate that $r_\Omega$ is at most of order unity due to the steep confining potential. A more shallow confining potential is achieved in split-gate wires [3–7]. Using the device specifications of ref. [5], one obtains values of $r_\Omega$ in the range $r_\Omega \approx 3$–$6$. It is not clear whether these values are large enough to result in spontaneous spin polarization. The ideal devices for observation of ferromagnetism would be ultra-clean wires with widely separated gates to provide the most shallow confining potential possible.

In conclusion, interactions lead to deviations from one-dimensionality in realistic quantum wires and, as a consequence, the Lieb-Mattis theorem no longer applies. We have shown that strong enough interactions induce a ferromagnetic ground state in a certain range of electron densities, where the electrons form a zig-zag Wigner crystal.

* * *

This work was supported by the US Department of Energy, Office of Science, under Contract No. W-31-109-ENG-38.

REFERENCES

[1] van Wees B. J. *et al.*, *Phys. Rev. Lett.*, **60** (1988) 848; Wharam D. A. *et al.*, *J. Phys. C*, **21** (1988) L209.
[2] Auslaender O. M. *et al.*, *Science*, **308** (2005) 88.
[3] Thomas K. J. *et al.*, *Phys. Rev. Lett.*, **77** (1996) 135.
[4] Kane B. E. *et al.*, *Appl. Phys. Lett.*, **72** (1998) 3506.
[5] Thomas K. J. *et al.*, *Phys. Rev. B*, **61** (2000) R13365.
[6] Reilly D. J. *et al.*, *Phys. Rev. Lett.*, **89** (2002) 246801.
[7] Morimoto T. *et al.*, *Appl. Phys. Lett.*, **82** (2003) 3952.

[8] Kristensen A. *et al.*, *Phys. Rev. B*, **62** (2000) 10950.
[9] Cronenwett S. *et al.*, *Phys. Rev. Lett.*, **88** (2002) 226805.
[10] de Picciotto R., Pfeiffer L. N., Baldwin K. W. and West K. W., *Phys. Rev. B*, **72** (2005) 033319.
[11] Rokhinson L. P. Pfeiffer L. N. and West K. W., cond-mat/0509448.
[12] Wang C.-K. and Berggren K.-F., *Phys. Rev. B*, **54** (1996) R14257.
[13] Spivak B. and Zhou F., *Phys. Rev. B*, **61** (2000) 16730.
[14] Lieb E. and Mattis D., *Phys. Rev.*, **125** (1962) 164.
[15] Tokura Y. and Khaetskii A., *Physica E*, **12** (2002) 711.
[16] Meir Y., Hirose K. and Wingreen N. S., *Phys. Rev. Lett.*, **89** (2002) 196802.
[17] Matveev K. A., *Phys. Rev. Lett.*, **92** (2004) 106801.
[18] In particular, the commonly cited "exception" to the theorem —the one-dimensional Hubbard model with next-nearest-neighbor hopping [19, 20]— has physical meaning only if the electrons are allowed to bypass the nearest site and hop to the next one by using a second dimension.
[19] Mattis D. C. and Peña R. E., *Phys. Rev. B*, **10** (1974) 1006.
[20] Daul S. and Noack R. M., *Phys. Rev. B*, **58** (1998) 2635.
[21] Unlike the case of higher dimensions, the long-range order in a one-dimensional Wigner crystal is smeared by quantum fluctuations, and only weak density correlations remain at large distances [22]. On the other hand, the coupling of electron spins is controlled by electron interactions at distances of order $1/n$ (see also [23]), where the picture of a one-dimensional Wigner crystal is applicable.
[22] Schulz H. J., *Phys. Rev. Lett.*, **71** (1993) 1864.
[23] The contribution of the spectator electrons saturates rapidly as their number is increased. This indicates that the destruction of *long-range order* in the quasi-one-dimensional Wigner crystal by quantum fluctuations will not affect our conclusions.
[24] Piacente G. *et al.*, *Phys. Rev. B*, **69** (2004) 045324.
[25] Majumdar C. K. and Ghosh D. K., *J. Math. Phys.*, **10** (1969) 1388; 1399.
[26] Haldane F. D. M., *Phys. Rev. B*, **25** (1982) R4925.
[27] Eggert S., *Phys. Rev. B*, **54** (1996) R9612.
[28] Thouless D. J., *Proc. Phys. Soc. London*, **86** (1965) 893.
[29] Roger M., *Phys. Rev. B*, **30** (1984) 6432.
[30] Bernu B., Candido L. and Ceperley D. M., *Phys. Rev. Lett.*, **86** (2001) 870.
[31] Voelker K. and Chakravarty S., *Phys. Rev. B*, **64** (2001) 235125.
[32] White S. R. and Affleck I., *Phys. Rev. B*, **54** (1996) 9862.
[33] Hamada T. *et al.*, *J. Phys. Soc. Jpn.*, **57** (1998) 1891.
[34] Allen D., Essler F. H. L. and Nersesyan A. A., *Phys. Rev. B*, **61** (2000) 8871.
[35] Itoi C. and Qin S., *Phys. Rev. B*, **63** (2001) 224423.
[36] Klironomos A. D., Meyer J. S. and Matveev K. A., unpublished.